Electroweak Interactions at LEP

Bruno Borgia
Dipartimento di Fisica, Università "La Sapienza", Roma.
INFN - Sezione di Roma

Invited talk at the SLAC Summer Institute, Topical Conference, July 16-27, 1990, Stanford, CA, USA

Introduction

Electroweak interactions at LEP are a subject based on a wealth of data, given the success of the CERN e^+e^- storage ring. I will report on the results from the four experiments, ALEPH, DELPHI, L3 and OPAL after the analysis of about 1/2 of the data collected in 1989 and 1990(*).

The review will cover the electroweak aspects of the process $e^+e^- \to Z^\circ \to f\bar{f}$ where the fermions can be either quarks or leptons. The analysis of experimental data is based on the determination of the cross section integrated on the solid angle and on the asymmetry of forward-backward leptons in the final state.

In this game the knowledge of the center mass energy is fundamental as the determination of the luminosity by which the event rate is normalized to compute the absolute cross section. Therefore a specific attention is given to these subjects.

Absolute energy of LEP

The dominant systematic errors influencing the Z° mass and total width derive from the knowledge of beam energy and luminosity. Beam energy is given in first instance from the field integral at the central orbit:

(*) This review is updated with the results available at the time of Singapore Conference.

$$E_b \propto \int_{2\pi R} B\,dl \ .$$

Then $$\frac{\Delta E}{E} \simeq \frac{\Delta B}{B} + \frac{\Delta R}{R} \ .$$

The length of the circumference, $2\pi R$, is derived with high precision from the RF acceleration frequency and from the determination of the central orbit. The error estimated on the circumference is about 0.6 mm while the frequency is known with a considerable better accuracy. Therefore the energy scale is determined by the magnetic field measurement and the relative error is $\sim 5 \cdot 10^{-4}$.

A second method uses protons trapped by the RF cavities in a different harmonic number h_p and in the same orbit of positrons, at the injection energy of 20 GeV. [1]

The speed of protons is simply given by

$$\beta = \frac{2\pi R\, f_{RF}}{h_p} \qquad \text{where the revolution frequency is} \quad f = \frac{f_{RF}}{h_p} \ .$$

The momentum error is

$$\frac{\Delta p}{p} = \gamma^2 \frac{\Delta\beta}{\beta}$$

and results to be $\leq 1 \cdot 10^{-4}$ at 20 GeV.

The main contribution to the final error comes from scaling the result from 20 GeV/c to 45 GeV/c. This correction is given by the flux difference at the two energies measured in the dipoles of the ring. Once all effects are considered, the absolute energy scale is known within $\pm$ 30 MeV. [2]

The best accuracy on the absolute energy will be obtained by the spin resonance method. After the transverse polarization of the electrons is built up and measured, depolarization is induced at the resonant frequency of spin precession by a perturbing field. Polarization is measured by the asymmetry in backscattered laser beam. The error is estimated to be $\pm$ 5 MeV, considering all possible systematic uncertainties and instabilities. [3]

Once the absolute energy of one setting is determined, it remains to evaluate the point to point reproducibility since each filling can be at a different nominal energy. A conservative upper limit to this systematic uncertainty of the central value is 10 MeV. The effect on M_Z is estimated to be $\pm$ 5 MeV and on the total width Γ_Z is $\pm$ 6 MeV, depending from the actual sharing of luminosities between each energy.

The intrinsic beam energy spread also introduces a small smearing of the resonant Z° cross section. At the accelerator operating conditions the beam has an energy dispersion of $\sigma/E_b = 7.5 \cdot 10^{-4}$ [4] the effect of which is a systematic widening of Γ_Z by 5 MeV.

Finally one should consider possible systematic differences in center mass energies between the four interaction regions. This uncertainty is estimated to be of the order of 1 MeV.

In conclusion the absolute energy scale of LEP will be eventually determined with an error of $\pm$ 7 MeV, directly applied on the Z° mass. All other uncertainties will contribute with a smaller scale error and with a systematic error on the total width Γ_Z of 6 MeV after the correction of -5 MeV is applied. It means that the relative error on the Z° mass can be as small as 10^{-4}, perhaps less, and on the total width of the order of 10^{-3}. At this level of accuracy, the interpretation of the measured Z° parameters should be undertaken with extreme care.

Luminosity measurements

All four experiments normalize the event rate by measuring the Bhabha cross section at small angles. The advantage of this method relies on the absolute prediction of the cross section in terms of QED graphs only, as the t channel at small angles is dominated by one photon exchange.

ALEPH, DELPHI and OPAL measure the scattering cross section starting from $\theta_{min} \sim 40$ - 60 mrad, while L3 measures from $\theta_{min} = 24$ mrad up to 70 mrad. This geometrical acceptance gives to L3 a factor ~ 3 more counting rate than the hadronic events at the Z° peak, while the other three experiments have a counting rate roughly equal to the Z° events.

Table 1 summarizes the main features of the monitors, with a list of the main systematic errors grouped under six headings.

Table 1 - Luminosity monitors

	ALEPH	DELPHI	L3	OPAL
θ_{min} - θ_{max} (m rad)	50 - 110	43 - 135	27 - 70	58 - 120
$\sigma_{visible}$ (nb)	27	33	96	18
Systematics (%)				
Theory (BABAMC)	0.7	1.0	0.7	1.0
Trigger ε	small	< 0.6	0.1	
Event selection	0.22	1.4	0.7	0.5
Geometry	0.95	0.5	0.6	1.0
Background	small	0.5	small	small
MC/calibration	0.6	< 0.6	0.6	0.4
Total	1.3	2.0	1.3	1.6

All four experiments use the BABAMC Montecarlo [5] to compute the accepted Bhabha cross section, and therefore they have a common systematic uncertainty deriving from the theoretical approximations used in this program. The effect of higher order contributions to the $O(\alpha)$ cross section is estimated in all experiment to be ± 1.0 % or less. No theoretical limitations exist to reduce further this error down to ± 0.3 % [6] or even less.

The finite statistics of Montecarlo simulation introduce a not negligible uncertainty that again can be reduced.

The next relevant error is due to the imperfect knowledge of the geometry of the luminosity monitor. Only with time we can verify if each experiment has reached the ultimate accuracy.

Trigger efficiency and background subtraction generally represent the smallest contribution to the systematic error.

To illustrate the above points, fig. 1 and 2 present detailed comparisons between MC and data showing the excellent agreement between them. Figure 3 shows an example of background evaluation, by plotting the events versus the collinearity angle of the two electrons. The background is evaluated by the events outside the region limited by the cuts $\Delta\phi \pm 10°$. Figure 4 illustrates the contribution to the cross section deriving from multiple photon emission. Only few events have both electrons with energy less than $\frac{\sqrt{s}}{2}$. Background starts to dominate below the line at 45°.

To reduce the uncertainty due to the cut at θ_{min}, DELPHI adopts a precise lead collimator. However the systematic error deriving from the accurate knowledge of the geometry is of the same order as the other experiments.

Figure 5 shows the sensitivity of the luminosity to the selection cuts for the L3 monitor.

At the end even in the most conservative case the total systematic error is about 2 %, while it seems possible to reduce it further at the level of ≤ 1%.

Z° parameters and the Standard Model

The e^+e^- annihilation at LEP energies proceeds through a resonant process that can be analytically described at the lowest order in general terms by a relativistic Breit-Wigner cross section. Therefore the derivation of the resonance parameters as the mass and total width from experimental data should be performed without explicit intervention of any specific model. This problem was resolved by the work of Borrelli, Consoli, Maiani, Sisto. [7] Similar results can be found in [8].

The resonant cross section can be expressed as

$$\sigma(s) \cong \frac{12\pi\,\Gamma_{ee}\,\Gamma_{ff}}{(s-M^2)^2 + \frac{s^2\,\Gamma^2}{M^2}} \left[\frac{s}{M^2} + R_f\,\frac{s-M^2}{M^2} + \frac{\Gamma}{M}\,I_f\right] + \sigma_\gamma^{cont.} \qquad (1)$$

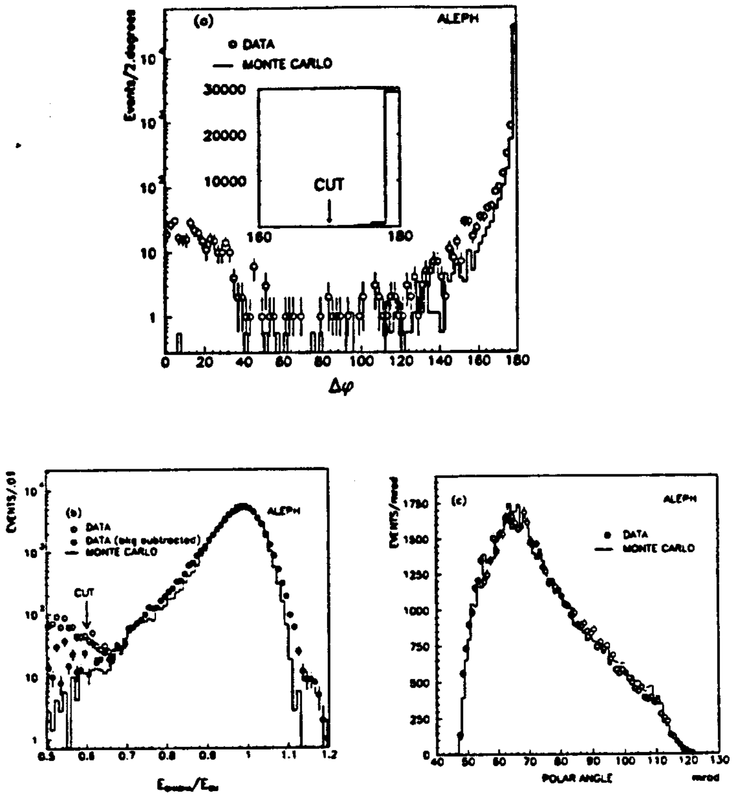

Fig. 1: Comparison between data and MC for the luminosity monitor of ALEPH.

a) Distribution of the difference in the azimuthal angle of e^+ and e^-.

b) Distribution of the total $e^+ + e^-$ energy before (open dots) and after (full dots) background subtraction.

c) Distribution of the polar angle of accepted events.

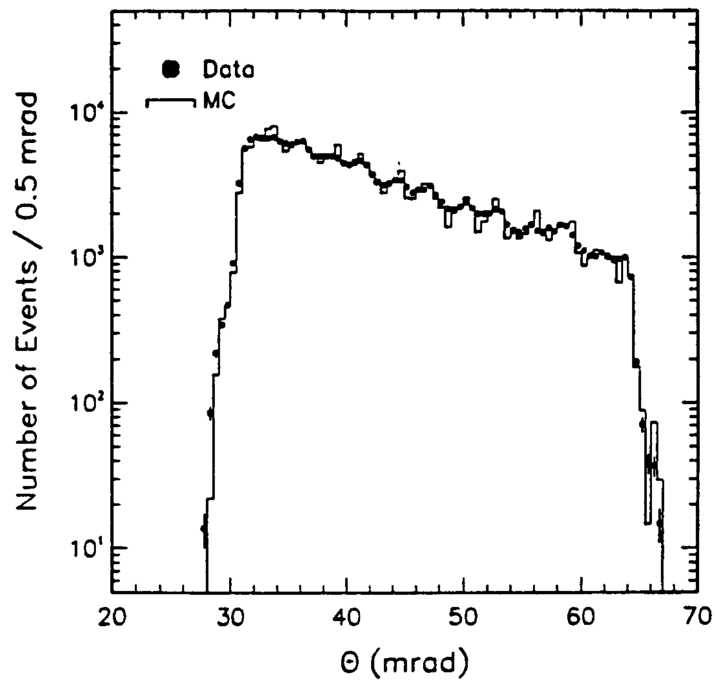

Fig. 2: Distribution of the polar angle for Bhabha events in one side of the luminosity monitor of L3.

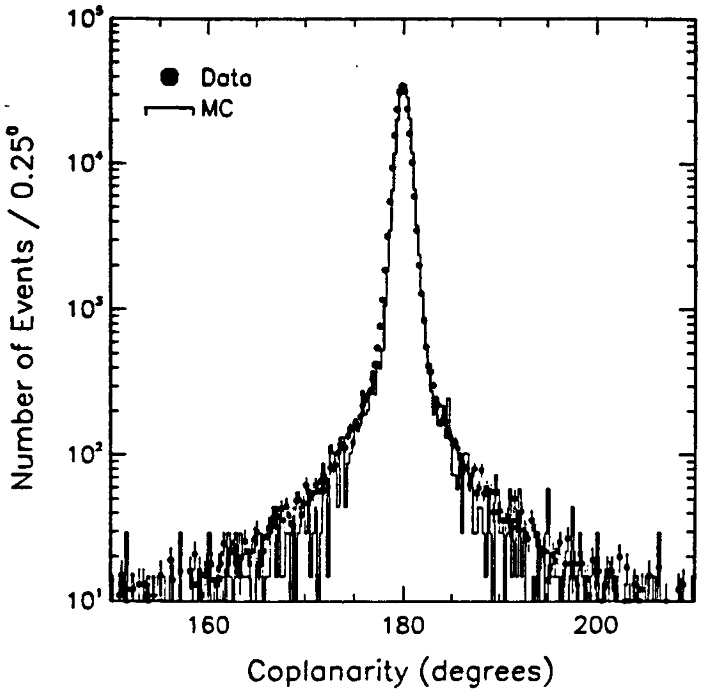

Fig. 3: Distribution of the azimuthal angle between e^+ and e^- for L3 monitor.

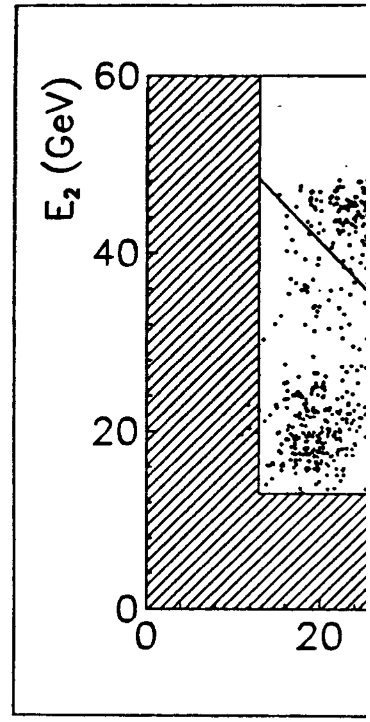

Fig. 4: Scatter plot of e^+e^- energies i
monitor. The shaded area is excl
energy. Events below the diagon

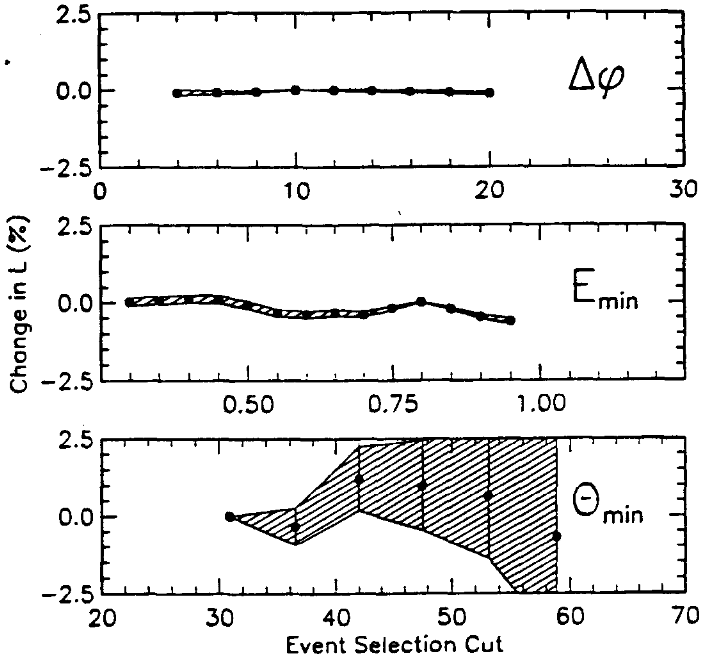

Fig. 5: Percentage change of luminosity from variation of cuts used in event selection for the L3 monitor.

where $M = Z^*$ mass,

$\Gamma = Z^*$ total width,

$\sigma_\gamma^{cont.}$ is the contribution from the one photon exchange diagram,

and R_f and I_f are small terms.

R_f is due to the interference of the resonance with the continuum due to photon exchange, and is affected by the presence of heavy states with mass larger than the Z^* mass.

I_f represents the absorptive contribution in the imaginary amplitude due to the known vector particle spectrum up to the Z^* mass. Its value can be computed and is of the order of 10^{-2}. Therefore the equation for the cross section of the process $e^+e^- \rightarrow f\bar{f}$ depends only from the parameters M, Γ, Γ_{ee} Γ_{ff} and R_f. Its precision is limited only by the truncation of the series expansion in $(s-M^2)/M^2$.

Finally the computation of the observed cross section is obtained by convoluting the expression (1) of the cross section with the initial center of mass energy spectrum after the photon radiation by the incoming electron or positron:

$$\sigma_{obs}(s) = \int_0^{1-x} H(x)\, \sigma\ [s(1-x)]\ dx \qquad x = s/s_0$$

where $\sqrt{s_0}$ is the minimum c.m. energy necessary to observe the final state, and H(x) is the initial state radiation spectrum.

The partial width Γ_{ff} in the Born approximation, assuming the exchange of one photon and of the Z^*, is simply given by:

$$\Gamma_{ff} = \frac{N_c\, G_F\, M_Z^3}{24\, \pi\sqrt{2}} \left(g_{Vf}^2 + g_{Af}^2\right)$$

where g_A and g_V are the coupling constants for the axial and vector currents.

Their values are further specified in the Standard Model in terms of the neutral current parameter sin θ_W as

$$g_{Vf} = 1 - 4\,|Q_f|\sin^2\theta_W\ ; \qquad g_{Af} = 1\ .$$

However the Born approximation is totally inadequate since higher order terms give a contribution larger than the present experimental accuracy.

These higher order graphs can be grouped in "QED corrections" having an additional real or virtual photon and in "Weak corrections." The last class includes propagator and vertex modifications to the Born diagram and box terms. The presence of the virtual top exchange gives a dependence from its mass to the radiative corrections. A smaller effect is due to the Higgs mass.

The consistency of all quantities computed by the Standard Model by using a unique value for the top mass is a very strong test of the renormalizibility of the theory.

In most cases the effect of radiative corrections can be accounted by a simplified expression of the complete theoretical formulae. This approach is known as "improved Born approximation." [9] The main features of this approach consist in replacing the couplings with effective quantities, and fixed constants with the running values at $s = M_Z^2$. As an example the partial width Γ_{ff} is

$$\Gamma_{ff} = \frac{N_c G_F \rho M_Z^3}{24 \pi \sqrt{2}} \left[1 + (1 - 4 |Q_f| \bar{s}^2)^2\right] \qquad (2)$$

where $N_c = 1 \cdot \left(1 + \frac{3\alpha}{4\pi} Q_f\right)$ for leptons

$= 3 \cdot \left(1 + \frac{3\alpha}{4\pi} Q_f\right)\left(1 + \frac{\alpha_s(M_Z^3)}{\pi}\right)$ for quarks

and $\rho \cong 1 + \delta\rho = 1 + \frac{3 G_F m_t^2}{8\pi^2 \sqrt{2}}$

$$\bar{s}^2 = \overline{\sin^2\theta_W} = \sin^2\theta_W + \cos^2\theta_W \, \delta\rho$$

having defined $\sin^2\theta_W = 1 - \frac{M_W^2}{M_Z^2}$ [10].

Asymmetry

The next physical quantity to consider beside the total cross section is the forward-backward or charge asymmetry. This quantity condenses the information given by the angular distribution of the process.

Recalling that the differential cross section derives its form by the exchange of a virtual Z^*, a photon and by their interference, its analytical expression in terms of the current couplings is:

$$\frac{d\sigma}{d\cos\theta} = \frac{\alpha^2}{4s}\left[1 + 2g_V^2 \, \mathrm{Re}(\chi) + \left(g_V^2 + g_A^2\right)^2 |\chi|^2\right]\left(1 + \cos^2\theta\right)$$

$$+ \left\{2 \, g_A^2 \, \mathrm{Re}\,(\chi) + 4 \, g_V^2 \, g_A^2\right\} \cdot 2\cos\theta$$

with $\chi = \frac{s}{s - M_Z^2 + i M_Z \Gamma_Z}$.

Therefore summing events with the final fermion having $\cos\theta > 0$ and events with $\cos\theta < 0$, we can measure the asymmetry

$$A_{FB} = \frac{\sigma_F - \sigma_B}{\sigma_F + \sigma_B} \; .$$

It is easy to see that while the total cross section is proportional to $\left(g_V^2 + g_A^2\right)^2$ the asymmetry is proportional to the product $g_V^2 \cdot g_A^2$. The two measurements then can provide these constants up to a sign ambiguity.

Experimental results and fits

Inclusive hadronic cross section and individual leptonic cross sections are measured by all four experiments [11] as shown in figures 6-9.

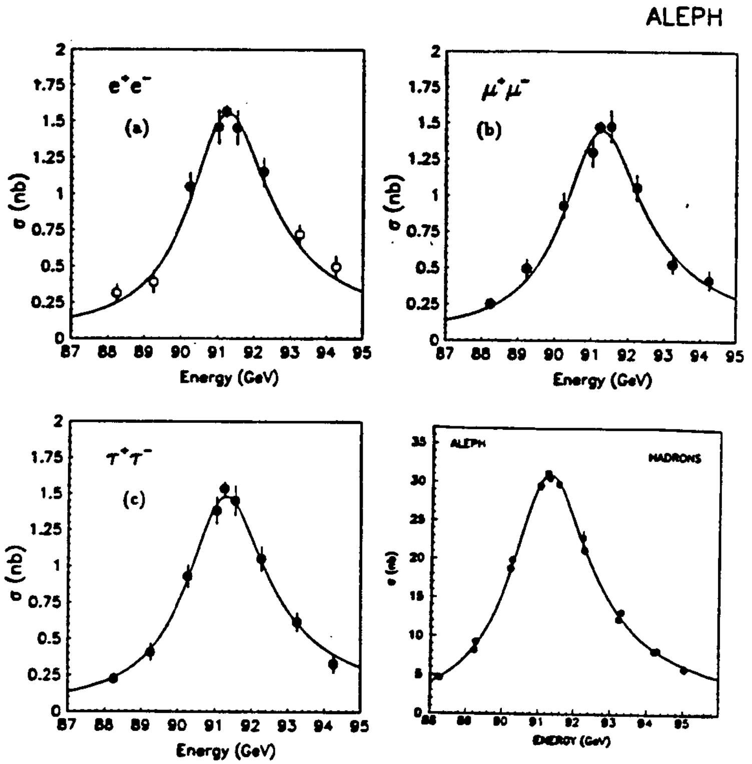

Fig. 6: Cross sections from ALEPH for $e^+e^- \rightarrow f\bar{f}$ as a function of the c.m. energy.
Final state: a) e^+e^-, b) $\mu^+\mu^-$, c) $\tau^+\tau^-$, d) hadron.
Full lines are the results of the fit with Burgers formula.

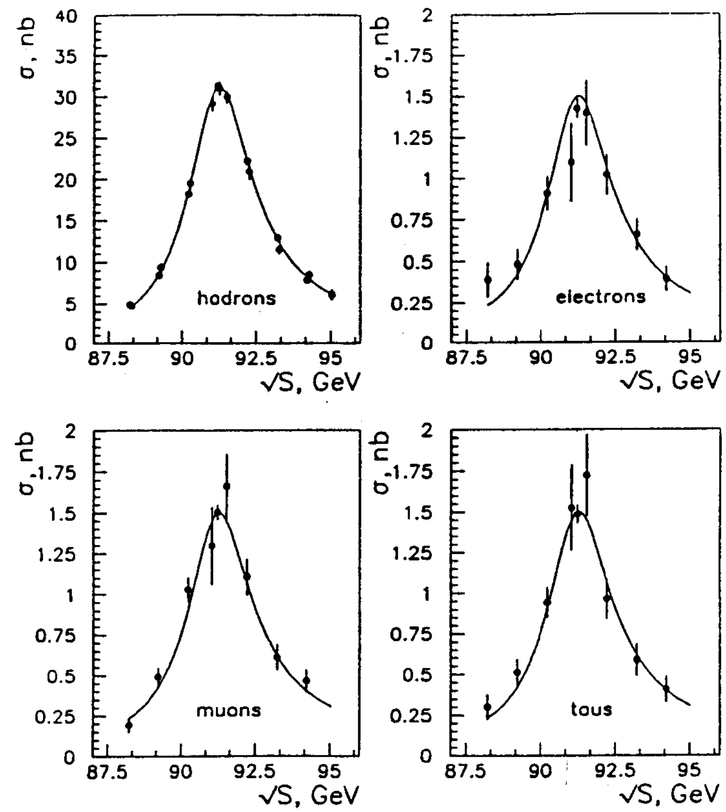

Fig. 7: Same of fig. 6 from DELPHI.
a) hadrons, b) e^+e^-, c) $\mu^+\mu^-$, d) $\tau^+\tau^-$.
The fit is performed with D. Bardin program.

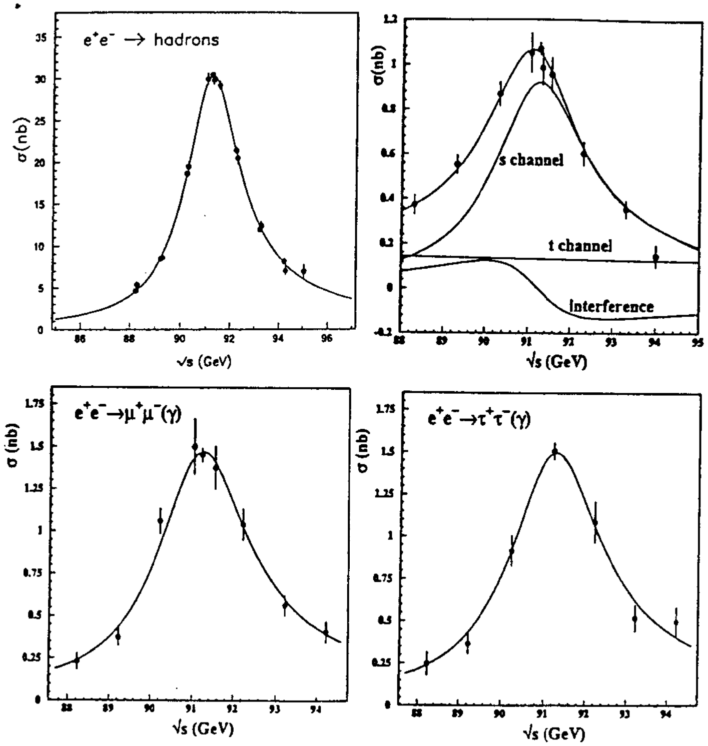

Fig. 8: Same of fig. 6 from L3.
a) hadrons, b) e^+e^-, c) $\mu^+\mu^-$, d) $\tau^+\tau^-$.
The fit uses Cahn formula except for the e^+e^-channel which is fitted with M. Greco. The contributions from the s and t channels are shown explicitly.

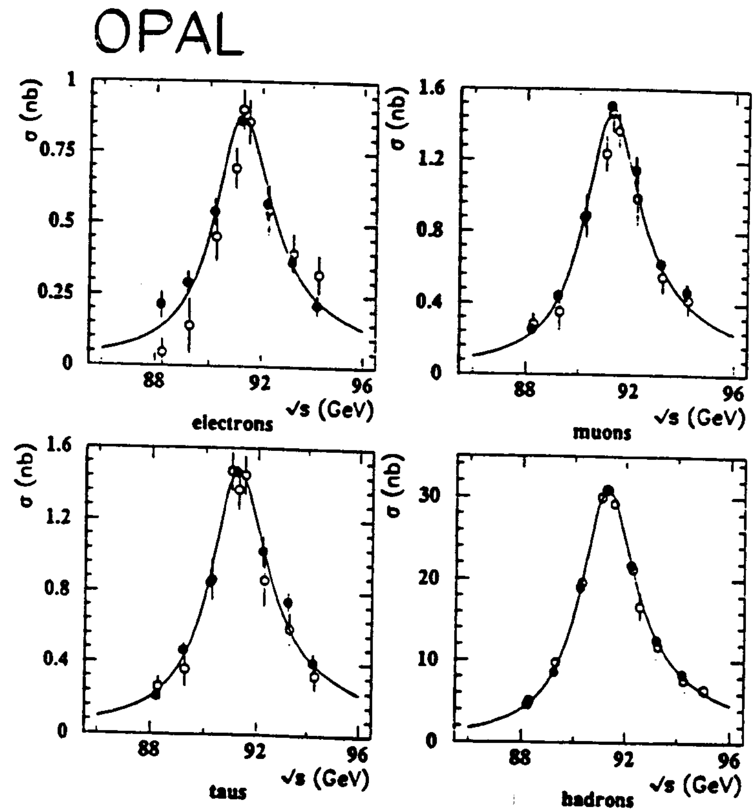

Fig. 9: Same of fig. 6 from OPAL.
a) e^+e^-, b) $\mu^+\mu^-$, c) $\tau^+\tau^-$, d) hadrons.
Fits are performed with D. Bardin program.
Open points: '89 data, full points: '90 data.

Since an excellent agreement exists between all measurements, the understanding of systematic errors is crucial to assess the impact of the present experimental results on the validity of the Standard Model. This consideration is even more relevant if one wants to combine the four experiments when all 1990 results will be available.

Table 2 summarizes the number of events collected in the leptonic and hadronic channels with some relevant features, while table 3 gives a list of systematic errors.

Table 2 - Main characteristics of events collected by LEP experiments

	ALEPH	DELPHI	L3	OPAL	Σ
$\int \mathcal{L}\,dt$ (pb^{-1})	2.5	3.3	2.9	5	13.7
hadrons	56 K	68 K	62 K	112 K	300 K
ε %	97.5	92.7	97.8	97.7	
e e	2404	1389	2642	3270	9705
$\cos\theta_{min}$ (e^-)	-0.9	-0.64	-0.74	-0.7	
$\cos\theta_{max}$ (e^-)	0.7	0.64	0.74	0.7	
μμ	1973	1618	1244	4642	9477
ττ	2169	1019	1169	3412	7769

Table 3 - Systematic errors for the various final states (%) and for the luminosity

	ALEPH	DELPHI	L3	OPAL
e e theory	0.5	1.0	0.7	0.5
e e total	1.0	1.3	1.2	1.0
μμ	0.9	1.9	1.3	0.9
ττ	1.7	2.7	3.0	1.9
hadrons	0.4	1.1	0.7	0.8
luminosity	1.3	2.0	1.3	1.6

All experiments have collected and analyzed so many events in the hadronic channel that the statistical error on the peak value of the cross section is considerably smaller than the systematic uncertainty. The contribution of the two types of error on the Z° parameters will be best appreciated after fitting the cross section to the experimental points.

Each collaboration fits the experimental data in a model independent way using only the hadronic cross sections or all three leptons and hadrons results in a global fit. The most straightforward comparison among the four experiment is given by the result of the fit to the hadronic cross section only, where the statistics is the highest and systematic errors are the smallest among the four possible channels. The free parameters usually are the Z° mass, the total width and the peak cross section σ_h^0. An equivalent choice is M_Z, Γ_Z and the product of the partial widths $\Gamma_{ee}\,\Gamma_h$. We can derive the three leptonic partial widths by also using the individual leptonic cross sections, and imposing the universality, we obtain the leptonic partial width.

ALEPH collaboration quotes results obtained by fitting the cross section with Burgers formula, DELPHI and OPAL use Bardin formula, while L3 uses Cahn or Borrelli. Differences in the results by using different formulas on the same data are smaller than the present individual experimental errors.

The ee(γ) channel requires a special treatment because of the presence of the t exchange diagram. L3 uses the improved calculation of Aversa, Greco et al. [12] This new calculation has a better factorization scheme and contains two-loop QED corrections. Hard photon emission is always computed in the collinear approximation. The partial width Γ_{ee} is extracted by fitting the experimental points with [12]. This procedure requires some kinematical cuts to reject events containing non collinear hard photons. L3 uses an acollinearity cut of $\Delta = 5^\circ$ between e^+ and e^-, and the emitted photon should be in a cone with an angle from the final $e^\pm$ not larger than $\delta = 5^\circ$.

DELPHI and OPAL compute the t channel contribution with the program ALIBABA of Beenakker et al. [13] that includes all one loop and box terms with leading log summation for photonic corrections. Non collinear hard photon emission is also explicitly computed.

Since the ALIBABA program is too slow to fit the data, only the t-channel contribution and its interference with the s-channel is evaluated and then subtracted from the measured cross section. The remaining cross section is then fitted as a pure s-channel contribution with Bardin formula. A similar technique was adopted by ALEPH collaboration, but since neither the improved Greco formula nor the ALIBABA program was available at the time of their publication, the t channel term was computed with the program of Caffo and Remiddi based on Greco previous work published in 1988, see reference 12.

From the above description clearly the ee(γ) final state should be studied further by comparing the results obtained by different kinematic cuts and theoretical approaches. Presently the statistical errors of each individual experiment are larger than the systematic ones.

Only one collaboration, OPAL, includes the asymmetries of the three lepton channels in the global fit. The other three collaborations derive from the asymmetry the $g_A^2\, g_V^2$ combination and with the leptonic width $\Gamma_{\ell\ell}$ a g_A g_V contour is obtained. In the framework of the Standard Model the parameters ρ and $\sin^2\bar{\theta}_W$ are also explicitely computed. The value $\sin^2\bar{\theta}_W$ in the minimal Standard Model is listed in table 4. Figures 10-13 illustrate the asymmetry measurements and fig. 14-15 give the contour plots g_A versus g_V while fig. 16 shows ρ versus $\sin^2\bar{\theta}_W$.

Table 4 - $\sin^2\bar{\theta}_W$ in the minimal Standard Model from the LEP experiments

ALEPH	DELPHI	L3	OPAL
0.2291 ± 0.0040	0.2309 ± 0.0048	0.230 ± 0.004	0.2315 ± 0.0028

Several authors combine the results of the four experiments either by computing weighted averages of the physical quantities [14] or fitting directly the cross sections. [15] The simple average of the final results does not consider that

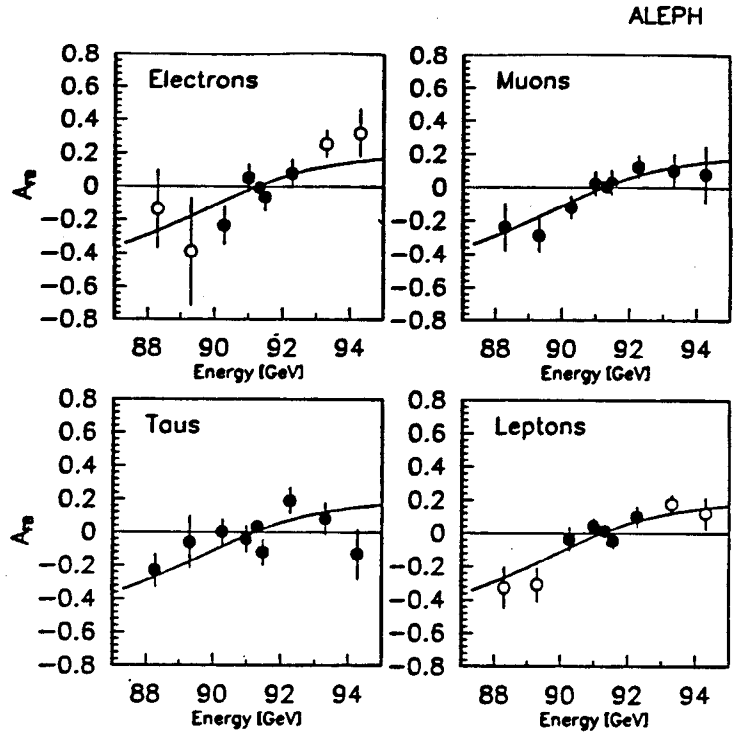

Fig. 10: Forward backward asymmetry A_{FB} from ALEPH.
a) e^+e^-, b) $\mu^+\mu^-$, c) $\tau^+\tau^-$, d) the flavour of the final state is ignored therefore "leptons" include electrons, muons and taus.

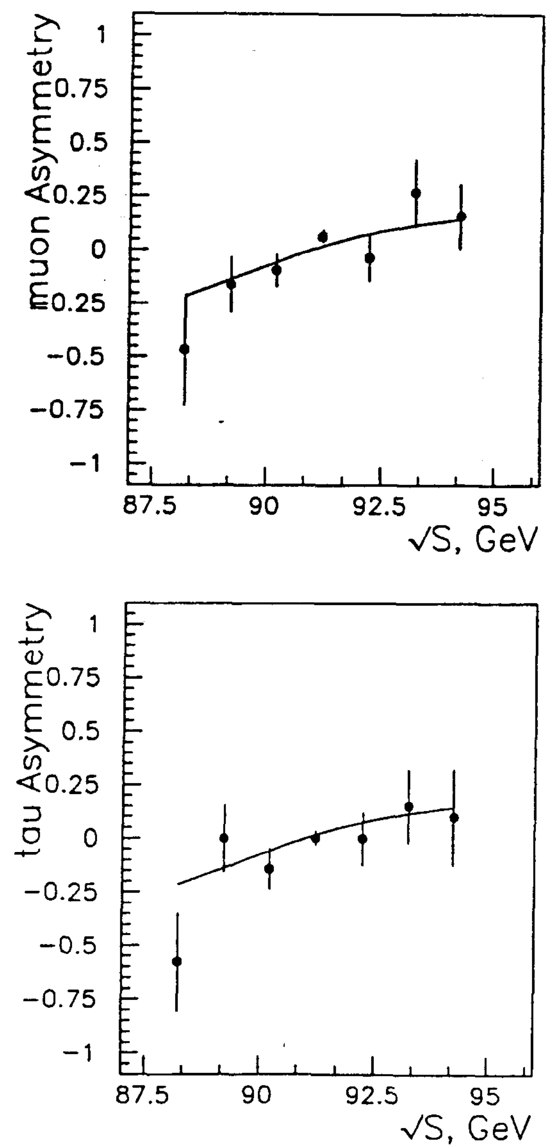

Fig. 11: Asymmetry A_{FB} from DELPHI. a) $\mu^+\mu^-$, b) $\tau^+\tau^-$.

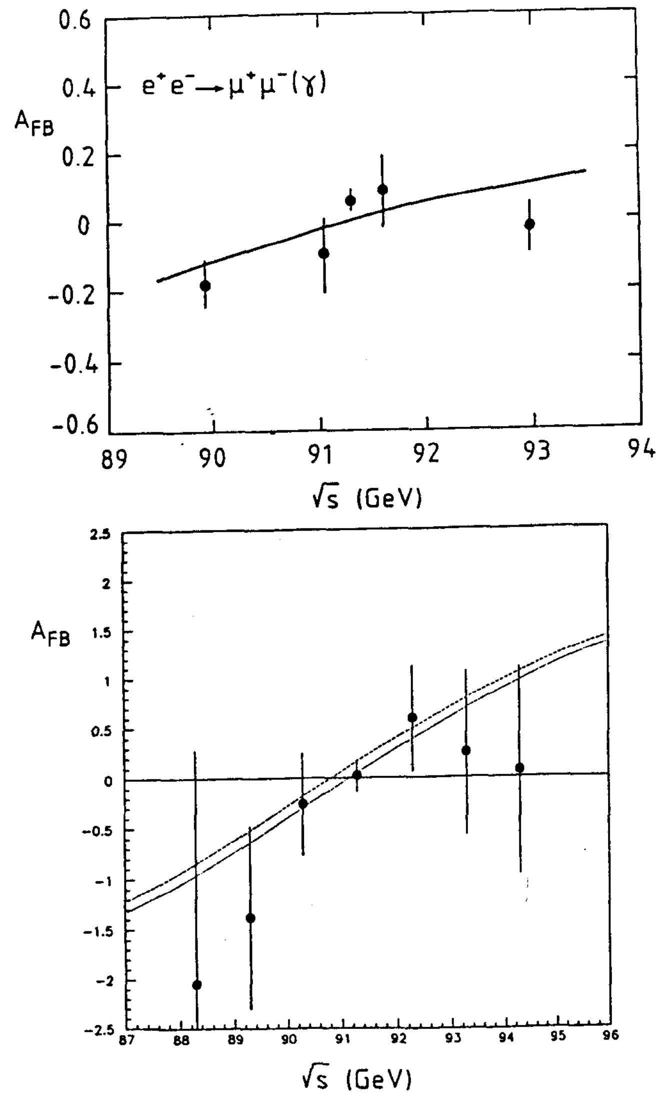

Fig. 12: Asymmetry A_{FB} from L3. a) $\mu^+\mu^-$, b) e^+e^-.

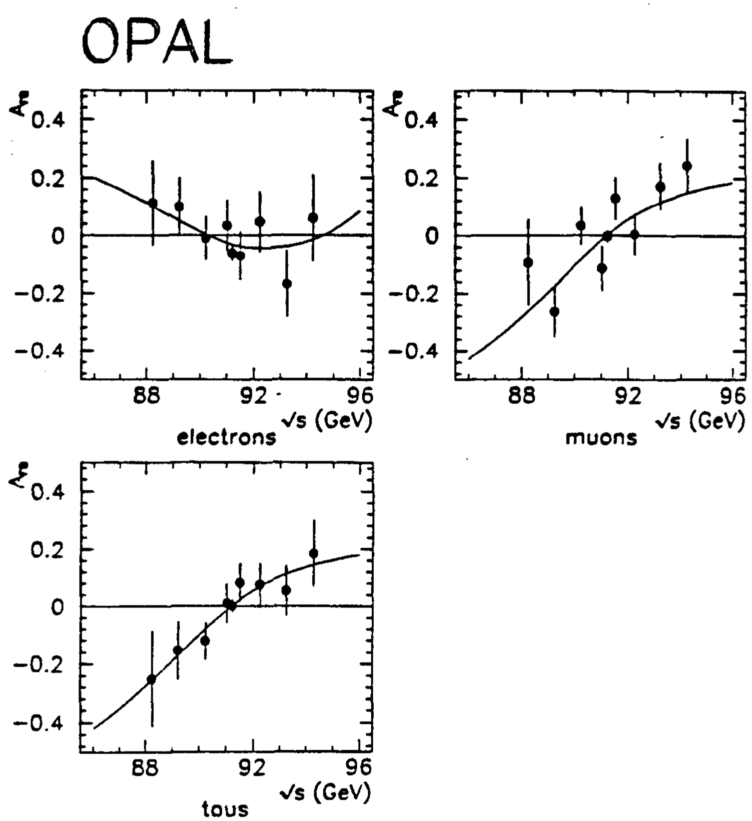

Fig. 13: Asymmetry A_{FB} from OPAL.
a) e^+e^- including the t channel contribution, b) $\mu^+\mu^-$, c) $\tau^+\tau^-$.

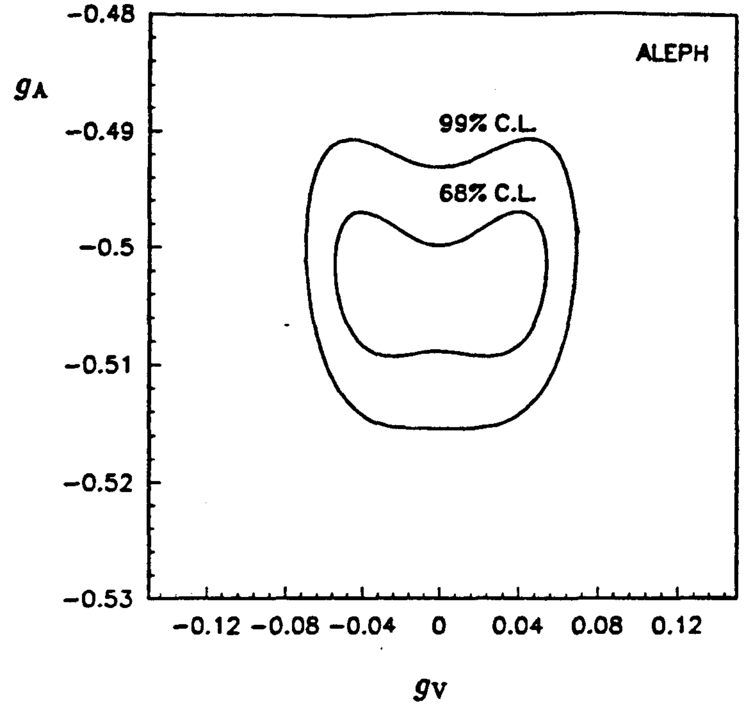

Fig. 14: Probability contours for $g_{V\ell}$ (M_Z^2) and $g_{A\ell}$ (M_Z^2). (ALEPH Collaboration).

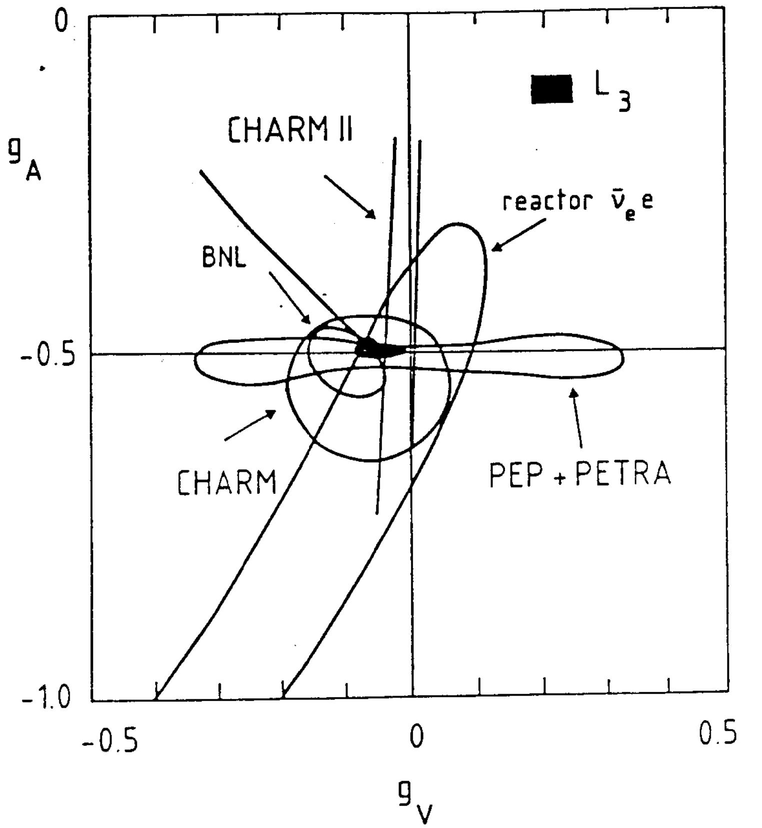

Fig. 15: $g_{V\ell}$ and $g_{A\ell}$ contours from neutrino experiments at 68% confidence level and low energy e^+e^- experiments at 95% confidence level. The shaded area represents the L3 measurement at 68% confidence level.

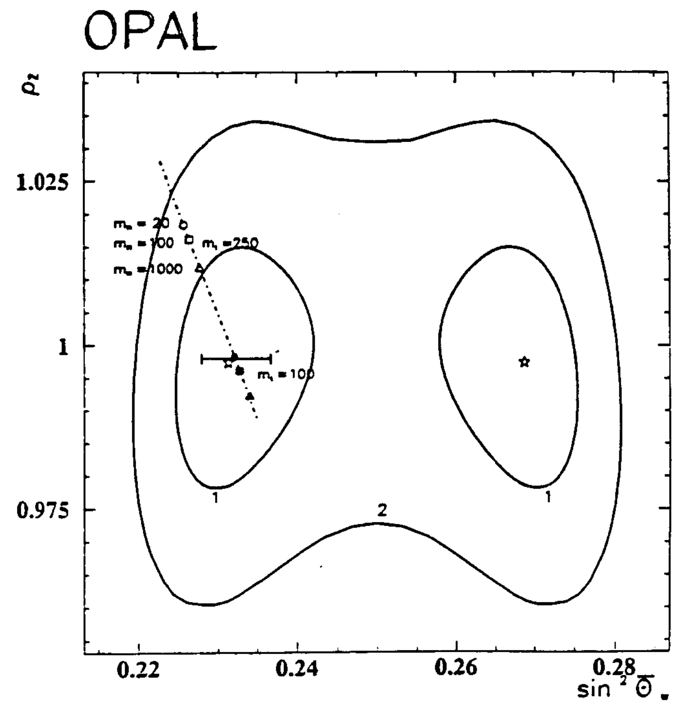

Fig. 16: One standard deviation confidence level contour in ρ vs $\sin^2\overline{\theta}_W$ from OPAL. The stars indicate the best fitted values. Various choices of m_t and m_H are shown on the line describing the Standard Model relation between ρ and $\sin^2\overline{\theta}_W$.

each collaboration uses different model independent formulae. Systematic errors and correlations must be treated ad hoc. It is evident that fitting directly the cross section points has the merit to use a consistent procedure for all experiments, provided the common systematic uncertainties are subtracted.

M. Diemoz and E. Longo performed this fit either using only the hadronic cross section or the hadronic, muon and τ cross sections. The electrons are not included because of the theoretical uncertainties explained above. The details of the procedure are discussed in [16]. They also evaluate carefully the effect of systematic errors of various origins, especially from the beam energy definition. The paragraph "Absolute energy of LEP" quotes in fact some of their results. Table 5 shows the results of this fit compared with the values published by each experiment under similar conditions.

Table 5 - Z° parameters

	M_Z (GeV) h only	Γ_Z (GeV) h only	Γ_h (MeV)	Γ_u (MeV)
ALEPH	91.193 ± 0.016	2.497 ± 0.031	1754 ± 27	84.3 ± 1.3
DELPHI	91.190 ± 0.014	2.466 ± 0.029	1756 ± 30	83.7 ± 1.4
L3	91.161 ± 0.013	2.492 ± 0.025	1748 ± 35	84.0 ± 1.2
OPAL	91.164 ± 0.011	2.496 ± 0.021	1778 ± 26	83.6 ± 1.0
"4 exp." ($h\mu\tau$)	91.171 ± 0.006 ± 0.030	2.485* ± 0.012	1756 ± 16	83.8 ± 0.7
SM m_t = 80-200 GeV m_H = 40-100 GeV α_s = 0.112 ± 0.10		2.486 ± 0.028	1735 ± 21	83.6 ± 0.7

* corrected by -5 MeV.

Standard Model interpretation

Among all possible quantities derived from the model independent fit, the peak cross section σ_h^0 and the ratio of the partial widths $R_h = \Gamma_h/\Gamma_{ll}$ are two of the least sensitive parameters to the top mass m_t and the Higgs mass m_H. Therefore they constitute an excellent test of the Standard Model. As shown in [17] the theoretical predictions for these are

$$\sigma_h^0 = \frac{12\,\pi}{M_Z^2}\;\frac{R_h}{(3 + 3\,\Gamma_\nu/\Gamma_{ll} + R_h)^2} = 41.3 \pm 0.15 \text{ nb} \quad \text{for } M_Z = 91.171 \text{ GeV}$$

$$R_h = \Gamma_h/\Gamma_{ee} = 20.75 \pm 0.12 \tag{3}$$

when the unknown parameters are allowed to vary between the following limits

$$\begin{aligned} m_t &= 80 - 200 \text{ GeV} \\ m_H &= 40 - 1000 \text{ GeV} \\ \alpha_s &= 0.112 \pm 0.010\,. \end{aligned} \tag{4}$$

Actually all uncertainty on R_h derives from the experimental error on α_s. In fact in the ratio of the partial widths the dependence from the top and Higgs masses cancels and the only surviving large correction derives from QCD, i.e.,

$$\Gamma_h = \Gamma_h^{(0)}\,(1.0375 \pm 0.0035)\ .$$

Therefore while $\Gamma_h^{(0)}/\Gamma_e = 20.00 \pm 0.03$, the ratio between effective quantities gives the value (3). The values obtained by the "4 experiments" fit are

$$\sigma_h^0 = (41.94 \pm 0.13 \text{ stat} \pm 0.35 \text{ syst}) \text{ nb} \qquad (M_Z = 91.171 \text{ GeV})$$
$$R_h = 20.94 \pm 0.17 \text{ stat} \pm 0.16 \text{ syst}$$

in excellent agreement with the predictions.

In the minimal Standard Model the mixing parameter $\sin^2\theta_W$ is a function of measured physical quantities and of the radiative corrections. Therefore one can compute [9] $\sin^2\theta_W$ either from the Z° mass or from the partial widths. For example formula (2) expresses one possible relation between Γ_{ff}, $\sin^2\theta_W$ and $\Delta\rho$. The explicit expression of the radiative corrections depends from the $\sin^2\theta_W$ definition and is a function of the unknown masses of the top and of the Higgs.

Defining

$$\sin^2\theta_W = 1 - \frac{M_W^2}{M_Z^2}$$

the hadron collider results [18] give the value $\sin^2\theta_W = .227 \pm 0.007$, while from the inelastic neutrino scattering νq [19] one obtains 0.231 ± 0.006.

In fig. 17-19 $\sin^2\theta_W$ [20] is plotted versus the top mass for the experimental values M_Z, Γ_Z, Γ_h and Γ_{ll} as derived from the 4 experiment fit.

All these quantities are consistent with a top mass $m_t = 150 \pm 20$ GeV.

Finally the number of light neutrino species can be obtained from the invisible width:

$$N_\nu = \Gamma_{inv}/\Gamma_\nu = \left[\Gamma_Z - \Gamma_h - 3\,\Gamma_{ll}\right]/\Gamma_\nu \quad .$$

Assuming the widths from the minimal Standard Model, the hadronic cross section can be fitted with the only free parameters M_Z and Γ_{inv}. This procedure gives obviously the smallest error. To derive a value with the minimum assumptions from the Standard Model, the above formula is rewritten as

$$N_\nu = \frac{\Gamma_{ll}}{\Gamma_\nu}\left[\left(\frac{12\pi\, R_h}{M_Z^2\,\sigma_h^0}\right)^{1/2} - R_h - 3\right]$$

where all quantities are measured except the ratio $\Gamma_{ll}/\Gamma_\nu = 0.5010 \pm 0.0005$ is taken from the Standard Model prediction. The error is given by theoretical uncertainties due to the unknown parameters listed in (4).

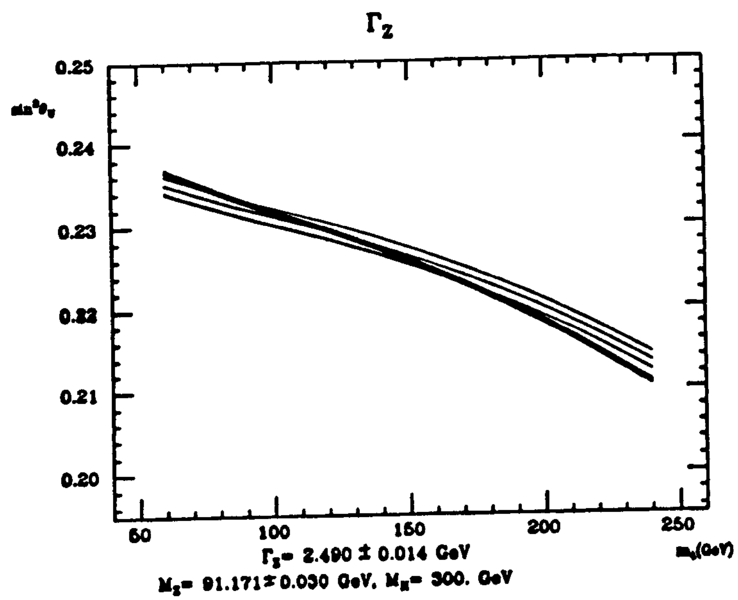

Fig. 17: $\sin^2\theta_W$ versus m_t for the experimental values of M_Z and Γ_Z fitted from the 4 experiments.

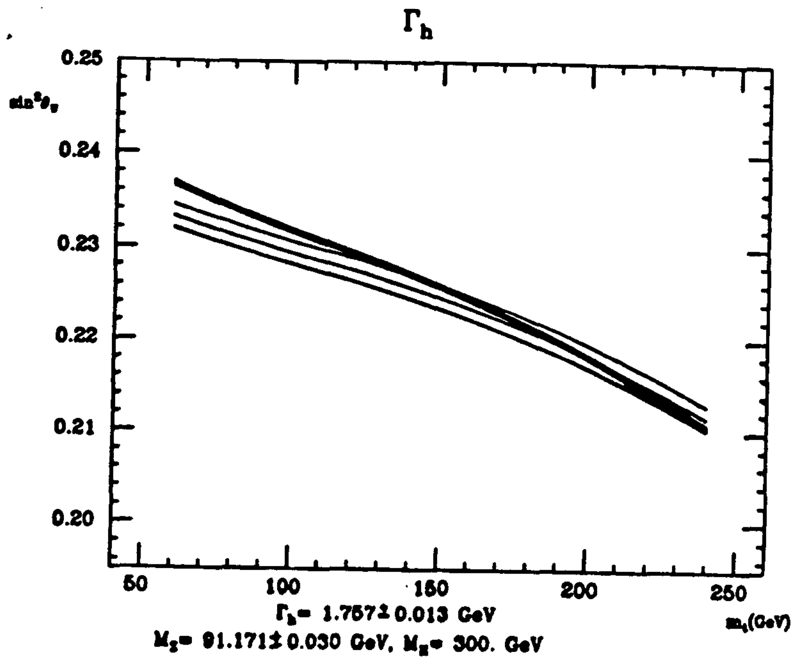

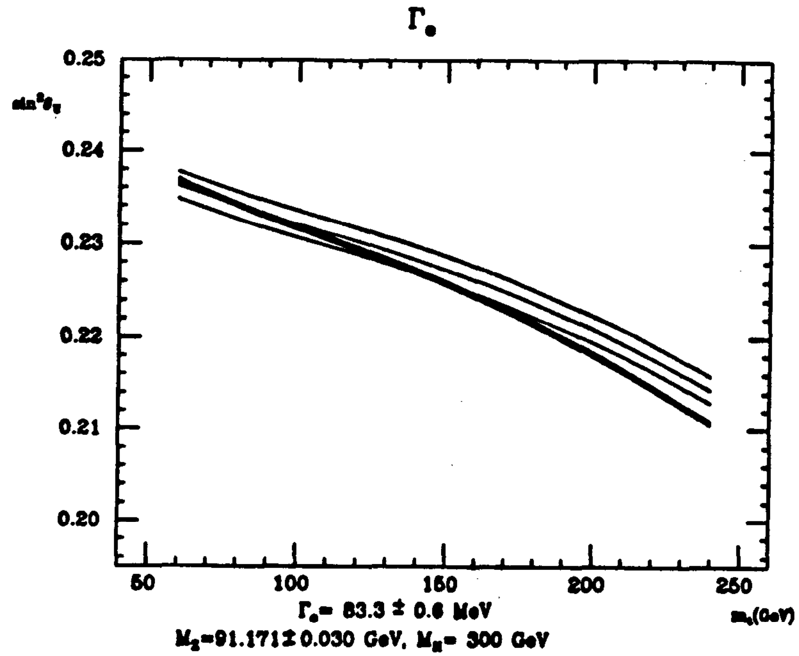

Fig. 18: Some plot as fig. 17 for M_Z and Γ_h.

Fig. 19: Some plot as fig. 17 for M_Z and $\Gamma_{\ell\ell}$.

Table 6 shows the values measured by each of the four experiments. The last column lists the free parameters actually used in the fit. The "4 experiments" fit uses M_Z, Γ_h, Γ_{ll} and Γ_{inv} as free parameters assuming from the Standard Model the value $\Gamma_{\nu\nu}$ = 167.3 ± 1.7 MeV. The error again is due to the unknown parameters. The number of light neutrinos is

$$N_\nu = 2.88 \pm 0.06 \ .$$

Table 6 - Number N_ν of light neutrinos

	N_ν	Free parameters
ALEPH	2.91 ± 0.13	M_Z, σ_h^0, R_h
DELPHI	2.82 ± 0.11 ± 0.13	M_Z, Γ_Z, Γ_h, Γ_{ll}
L3	3.01 ± 0.11	M_Z, Γ_{inv}
OPAL	2.86 ± 0.15	M_Z, Γ_Z, Γ_h, Γ_{ll}

Conclusions

In the first year of operation LEP has produced already fundamental results reaching an unpredicted accuracy. The electroweak sector of the Standard Model is now established with a knowledge of the electroweak parameters at the percent level or better. If one combines the data from all experiments, the Z° parameters are:

$$M_Z = 91.171 \pm 0.006\ (\pm 0.030)\ \text{GeV}$$
$$\Gamma_Z = 2.489 \pm 0.012\ (-\ 0.004)\ \text{GeV}$$
$$\Gamma_{ll} = 83.8 \pm 0.7\ \text{MeV}$$
$$\Gamma_h = 1756 \pm 16\ \text{MeV}$$
$$N_\nu = 2.88 \pm 0.06$$

where the errors are the combination of statistical and systematic uncertainties.

LEP measurements and other electroweak results are consistent with a high top mass of about 150 GeV.

The next significative constraint to the Standard Model will be given by the W mass measurement at LEP 200, where it should be measured with an error of 100 MeV. At this level of accuracy, radiative corrections will be sensitive not only to the top but also to the Higgs mass.

Acknowledgments

I like to thank G. Feldman and the organizers of the SLAC Summer Institute for the invitation to the Conference.

I wish to acknowledge the collaboration of J. Lefrançois, T. Mori, P. N. Ratoff, L. Rolandi for clarifying conversations on the results from ALEPH, DELPHI and OPAL experiments. Discussions with M. Consoli and L. Maiani on the Standard Model predictions, with A. Hofmann and M. Placidi on LEP parameters were greatly beneficial.

A special thanks to my colleagues of L3 collaboration that helped me in the preparation of this review. Finally I am in debt to M. Diemoz and E. Longo for a critical reading of the manuscript.

References

[1] A. Hofmann, T. Risselada, LEP Note 383, 11.6.1982.

[2] R. Bailey et al., LEP energy calibration CERN SL/90-95.

[3] M. Placidi, R. Rossmanith, LEP-BI/86-25.

[4] A. Hofmann, private communication. For the effect on M_Z and Γ_Z see [16].

[5] M. Böhm, A. Denner, W. Hollik, Nucl. Phys. **B304** (1988) 687;
F. A. Berends, R. Kleiss, W. Hollik, Nucl. Phys. **B304** (1988) 712;
R. Kleiss in "Proceedings of the Workshop on Z Physics at LEP" CERN Report 89-08 (1989) **Vol. 3**, p. 88.

[6] R. Kleiss in "Z Physics at LEP1" CERN 89-08 **Vol. 3**, p.92.

[7] A. Borrelli, M. Consoli, L. Maiani, R. Sisto, Nucl. Phys. **B333** (1990) 357.

[8] D. Bardin, et al., Z. Phys. **C44** (1989) 493 and Comp. Phys. Comm. **59** (1990) 303;
F. A. Berends et al., " Z Physics at LEP" CERN 89-08 **Vol. 1**, p. 89;
F. A. Berends, G. Burgers and W. L. Neerven, Nucl. Phys. **B297** (1988) 429 and Nucl. Phys. **B304** (1988) 921;
R. N. Cahn, Phys. Rev. **D36** (1987) 2666.

[9] M. Consoli, W. Hollik in "Z Physics at LEP" CERN 89-09, **Vol. 1**, p. 7.

[10] A. Sirlin, Phys. Rev. **D22**(1989) 971;
W. Marciano, A. Sirlin, Phys. Rev. **D22**(1980) 2695.

[11] D. Decamp et al., ALEPH Collaboration, CERN-PPE/90-104 (19 July 1990);
P. Abren et al., DELPHI Collaboration, CERN-PPE/90-119 (16 August 1990);
B. Adeva et al., L3 Collaboration, L3 preprint # 09 (14 July 1990);
B. Adeva et al., L3 Collaboration, L3 preprint # 017 (20 August1990);
M. Z. Akrawy, OPAL Collaboration, OPAL Physics Note 90-16 (29 July 1990).

[12] M. Greco, Phys. Lett. **B171** (1986) 97;
M. Greco, Riv. Nuovo Cimento **11** (1988) 1;
M. Caffo, E. Remiddi, F. Semeria, "Z Physics at LEP" CERN 89-09 **Vol. 1**, (1989) p. 171;
F. Aversa, M. Greco, G. Montagna, O. Nicrosini, LNF-90/049 (PT) (12 July 1990).

[13] W. Beenakker, F. A. Berends, S. C. van der Marck, Leiden preprint (15 June 1990).

[14] L. Rolandi, CERN-EP/90-64;
E. Fernandez, CERN-PPE/90-151.

[15] S. Ganguli, CERN-PRE 89-062;
M. Consoli, C. Dionisi, L. Ludovici, Proceedings of "Les Recontres de la Vallée d'Aosta" La Thuile, Italy 1990.

[16] M. Diemoz, E. Longo, in preparation.

[17] M. Consoli, C. Dionisi, L. Ludovici, Proceedings of "Les Recontres de la Vallée d'Aosta" La Thuile, Italy 1990.

[18] J. Alitti et al., UA2 Collaboration, Phys. Lett. **B241** (1990) 150;
P. Schlabach, CDF Collaboration Proceedings of the APS Conference, Washington DC, April 1990.

[19] H. Abramowicz et al, CDHS Collaboration, Phys. Rev. Lett. **57** (1986) 298;
A.Blondel et al., Z. Phys. **C45** (1990) 361;
J.V. Allaby et al., CHARM Collaboration, Phys. Lett. **B177** (1986) 446 and Z. Phys. **C36** (1987) 611.

[20] A. Borrelli, L. Maiani, private communication.